McGill Physical Journal

Final Report on the Mössbauer Research Project for PHYS-396

Supervisor: Dr. Dominic H. Ryan, Student: Didar Sedghi (261002363)

McGill University Department of Physics

December 31, 2022

Abstract

This paper explores a novel way of collecting and analyzing Mössbauer absorption spectrum data as introduced by the paper [1]. The objective being that the proposed way of collecting data and using the statistical analysis tools presented in this Greek paper, one can construct an algorithm software to filter out the background contribution from any Mössbauer absorption spectrum. This algorithm was not constructed successfully in this paper, however all the ideas leading up to this algorithm were explored, and an assessment was made in regards to the fact that the new method of collecting data seems to provide more flexibility to manipulate said data compared to the conventional method of Mössbauer data collection which does not provide the same amount of leg room for specific channel analysis. The new method therefore offers a great potential for a better analyzing of Mössbauer experiments.

1 Introduction and Theory

1.1 Intro and Preface

This paper explores an alternative method of collecting and analyzing Mössbauer spectroscopy data. In order to therefore understand the main content of this paper, it is important to understand what Mössbauer spectroscopy is in the first place and to grasp the basic concepts of the Mössbauer effect in which this spectroscopic technique is based on. There are many different techniques which are based on this effect used in both scientific research and application. For the purpose of this introduction and paper, we focus on the most prominent technique; that of conventional Mössbauer spectroscopy in transmission geometry which will be discussed in-depth in the later part of this introduction.

1.2 The Mössbauer Effect

Gamma rays are a type of electromagnetic radiation that come about from the radioactive decay of atomic nuclei. More specifically, gamma rays are a result of nuclear transition in an atom from an unstable high-energy state to a stable low-energy state. Just as when shooting a gun causes a recoil due to the conservation of momentum, the same principle affects the emission of gamma rays from unstable high-energy state atomic nuclei. Going with the gun analogy, the unstable atom "shoots" the gamma ray and like a gun, the "shooting" atom recoils. That is to say, when an atom emits a gamma ray, just like a gun there is an associated recoil energy. The energy of this emitted gamma ray equals the energy of the nuclear transition, (going from high-energy to low-energy state), minus a contribution from the recoil energy that is lost when the atom emits the gamma ray. We can show this mathematically by

$$E_\gamma = E_{trans} - \rho_{recoil}, \tag{1}$$

where E_γ is the gamma ray energy, E_{trans} is the nuclear transition energy and ρ_{recoil} is the corresponding recoil energy. In the case where the lost recoil energy is very minuscule and small in comparison to the nuclear transition energy, we note that the gamma ray energy

will roughly equal to the nuclear transition energy ($E_\gamma \approx E_{trans}$). We often name such a phenomena as recoil-less or recoil-free. As such, we can claim that the gamma ray energy corresponds to the nuclear transition energy of the atom we are dealing with. This results in the capacity for this emitted gamma ray to be absorbed by a second atom of the same exact type as the one that emitted the ray. The absorption of the gamma ray by the same atom causes what we call resonance.

Typically in a gas atom, recoil energy is much higher which usually prevents such resonance events to occur. However, for solid atoms, the atomic nuclei is confined in a lattice structure. In the event of a gamma ray emission of a nuclei in a lattice structure, the lattice is caused to vibrate, however the recoil energy in such a case becomes negligible. Therefore we have a recoil-free event. In essence, the energy of the radioactive decay is either absorbed or given by the lattice of the matter, and the quantisation of this energy is called a phonon. It is specifically during these no phonon events which the Mössbauer effect is possible. The lattice crystals become the recoiling body and thus in such recoil-free events, the recoil energy is negligible; hence the emitted gamma rays have the appropriate amount of energy to be absorbed by the same atom in a fashion where resonance can be observed. In other words, during recoil-free events the lattice crystal structure vibrates absorbing the recoil making the recoil energy negligible and thus the energy of the gamma ray corresponds to the energy of the nuclear transition, allowing it to be absorbed completely by a second atom of the same type.

1.3 Mössbauer Spectroscopy

With the basic principle of the Mössbauer effect understood, we can now proceed to explain how this effect can be used as a spectroscopic technique. In this experiment, the utilized radioactive source is a ^{57}Fe. The sample also has to be of the same type of isotope as explained previously in the Mössbauer effect paragraph. The setup involves the main radioactive source emitting gamma rays and another sample some distance away being exposed to the source gamma radiation. The sample is placed in front of a detector that absorbs the incoming radiation through the sample with the intention of measuring the intensity of the radiation beam. The source itself is placed on a mechanically oscillating device which varies the speed

of the source. In essence, we expect a spectra graph that shows and plots the intensity of absorbed radiation by the gamma detector versus the different velocities. These different velocity values have been binned into "channels" as will be observed later on in the paper. So each channel value is attributed to different velocities the source attains by the fact that it is in motion due to the linearly accelerating motor.

If for a given channel the sample absorbs most of the incoming radiation beam (resonance), then the gamma detector will detect less intensity. For other channels, the sample may not absorb a lot of the beam, and as such the detector will indicate a higher intensity for those channels. The expected spectra is therefore in a form where there will be "dips" associated to the points in which most of the gamma radiation has been absorbed by the sample owing to the Mössbauer effect. This can be seen in figure 13

1.4 Experiment Objective

The main objective of this experiment and paper is to perform the new method of collecting Mössbauer data, and conduct the same statistical analysis done in the Greek paper [1]. The focus would be put on understanding in more depth what each of the new statistical modelling and estimations presented have to offer; with the ultimate goal being to put together all these different tools and to see if it is possible to reconstruct the algorithm system mentioned in the Greek paper for background filtering of Mössbauer absorption spectrum.

The proposed algorithm, named ALGO by the Greek paper, is claimed to be able to filter out the background contribution that can be found in Mössbauer spectra. This can be made more clear mathematically by the following equation

$$N(v) = BG - A(v), \tag{2}$$

where $N(v)$ is the variable for the real raw data measured in the experiment by the detection of counts (gamma photons as pulsed by the detector) at certain velocities v, where v is the previously discussed velocities of the radioactive source. The variable BG represents the background contribution from recoilless and non-recoilless γ-rays. In essence, the attempt is to try to divorce the noise and background of BG using the filter, to form a clearer spectrum.

2 Methods of Experimentation

2.1 Conventional Mössbauer Experiment

The conventional experiment for acquiring a Mössbauer absorption spectrum involves using a linearly accelerated motor, a radioactive source, a sample and a γ-ray detector placed behind the sample. The radioactive source is put in a constant acceleration by the linearly accelerated motor which moves the source relative to the sample to achieve different velocity values. The γ photon detector will consider each radiation detection coming from the γ beam as an event. These radiation detection events will be called counts. These counts will be represented, graphically, on the y-axis of the Mössbauer absorption spectrum, which effectively represents the intensity of the γ beam coming from the radioactive source; as more counts (radiation detection) represent a higher intensity and less counts represent a lower intensity. As mentioned previously, the source is in motion and attains different velocity values relative to the sample. The velocity values in this experiment are represented by "channels" which are found on the x-axis of the Mössbauer absorption spectrum. The different channels represent momentary velocities the source attains with respect to the sample. The channel values start from channel 0 to channel 511, which as mentioned represent different velcoity values of the source. In essence, the Mössbauer absorption spectrum that is formed (13) as the time evolves is the result of the accumulation of the counts for each individual channel. In other words, each channel simply adds the counts and accumulates them as the measuring time evolves. In such a fashion, the experiment starts when we allow the detector to start counting the radiation events and let the experiment run for a period of time; after a long time is passed, the spectrum is formed as each channel has its counts accumulated over the whole experimental period.

2.2 New Method

The new method [1] involves the same mechanical experimentation setup as before. However, the way in which the data is collected and later analyzed differs slightly. As mentioned previously, the conventional method simply requires that the experiment run for a certain

period of time and the counts to accumulate for each channel over that period of time, after which an end is put in the data collection and a final absorption spectrum is obtained.

In this new method, a given average count rate (CR) per channel is chosen as a target. This CR value represents in essence the average or mean counts per time interval per channel (CR = SOC/TI, where SOC stands for sum of counts, TI stands for time interval and CR for count rate). In the conventional experiment, the data collection simply starts by letting the photon detector start absorbing incoming beams and then after when a long period of time has passed the detection is put to an end, where finally a spectrum is acquired.

For the new method, the data collection is done in discrete steps. Firstly, for a specific CR target a number of sample runs are taken until the spectrum associated with these sample runs show that each channel has an average count rate corresponding to the target CR. For each run using the MCS software (this is the software in which the data collection is done), an associated time value called a "pass" is to be found, which represents the total time taken for any given run. Using a few simple lines of code, the MCS is commanded to then do a run with the pass found to form a spectrum having an average CR corresponding to the target CR. After a run is executed using the pass given by the code, the data is saved both in a .MCS file for a spectrum of the run and an .ASCII file for the numerical data of the run. The spectrum is cleared and another run is repeated with the same pass time; the data for this run is again saved in a similar fashion as before. This is repeated over and over until the desired time period, usually in the 24 hour range, is reached. With the conventional method, the size of the data is much smaller for the simple fact that only one run is done and the output is a single spectrum and a single data set. Since the new data collection involves discrete steps and which each step (or run) a data set is saved and this process is done over a long period of time, the final data bulk will usually be in the thousands or tens of thousands of files with the total file size reaching around 10 MB or more. An advantage that can be observed immediately with the discrete nature of data collection is that one can recreate a spectrum for any given time interval.

3 Results

The results will be presented in a linear manner showcasing the steps taken to reach the necessary tools needed for building the final algorithm. Each result is presented by itself with the intention to showcase the foundation needed for the desired ALGO program at the end while explaining the pertinence of the given result. Furthermore, each result is put in comparison with the result in the original paper which will act as a reference. Besides the main goal of investigating the claims of the paper regarding the background filtering algorithm, each tool needed to build the final ALGO program will also have something of value to give which will be detailed for all the tools.

3.1 The Mean-fit-Poisson "MFP"

The first statistical method presented here is the Mean-fit-Poisson, abbreviated to MFP for brevity's sake. The simple idea behind this is that since a mean or average count rate CR of μ=8 counts/TI was chosen for the experimental run, then it is expected that each channel have a mean of 8 counts/TI to occur for most of the absorption time period. In other words, the occurrence of an average of around μ=8 counts/TI for all 512 channels is expected since this is how the experiment was set up in the first place. Since radioactive decays follow a Poisson function, it would also be expected that the occurrence graph of the CRs to also follow a Poisson function. In this end, we therefore expect that low count rates and very high count rates to have low occurrences, whilst CRs around μ=8 counts/TI to have much higher occurrences; with the average of the Poisson graph to be peaked at about $\approx$ 8 counts/TI.

This can be clearly observed in figures 1, 2, and 3. In figure 1(a) channel 50 is a random channel picked to simply showcase that a background contribution channel achieved the mean CR occurrence; with the most occurrence of the CR being an average of 8.74 counts/TI. The occurrence graph in figure 1(b) is a specific absorption channel for channel 93, showcasing again that as expected, the mean count rate was indeed approximately close to 8 counts/TI. Four more absorption channels, channel 119, 191, 325 and 397 are also shown, again with the purpose to present that the highest occurrence of CR was close to the targeted mean of 8 counts/TI. These results are not spectacular in and of itself, since surely if the experiment

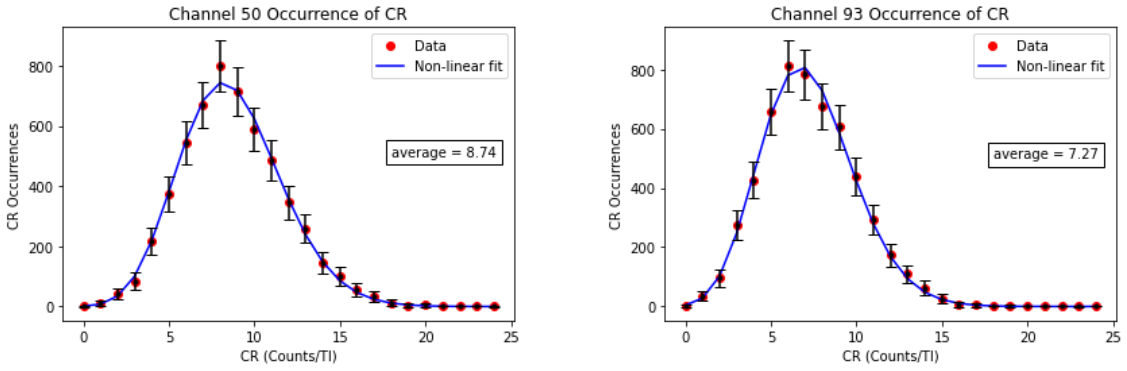

(a) (b)

Figure 1: CR occurrences as a function of CR for the μ=8 counts/TI average experimental run (a) channel 50 with μ=8.74 $\pm$ 0.10 counts/TI (background contribution channel) and (b) channel 93 with μ=7.27 $\pm$ 0.11 counts/TI (channel corresponding to an absorption dip in the spectrum). The y-axis is the value corresponding to the occurrences of count rates CR as a function of CR and the x-axis is the different values of CR that happened within that specific channel. As can be clearly noted, for both graphs their averages rest around μ=8 counts/TI, which makes sense since this was the targeted average for the experimental run. The blue line is the non-linear Poisson fit of the data and the black error bars are scaled by 3 to make them visible.

was set up properly with the intention of achieving a mean of 8 counts/TI per channel, then the occurrence of $\approx$ 8 counts/TI would be the highest for every channel. Despite the trivial nature of these graphs and results, it provides a succinct and clean way of observing what is happening in each channel; this is further reinforced by the fact that as expected, the occurrence graph follows a Poisson function as it should for a radioactive decay. The results from these occurrences graphs can be compared to that in the Greek paper as seen in figure 8.

Following the fact that the occurrence of CR as a function of CR for every channel follows a Poisson function, it is very reasonable then to perform a non-linear fit of a Poisson fit through the data points. This non-linear fitting procedure is then done on every single channel for all 512 channels. As can be observed individually for the channels 50, 93, 119, 191, 325 and 397, the blue line represents this very Poisson fit. Therefore after applying this non-linear fitting of Poisson fits, we end up with the result in figure 4. We showcased, individually, 6 channels with their corresponding occurrence graphs and Poisson non-linear fits; here in figure 4 we simply put together all the Poisson fits unique to each channel on

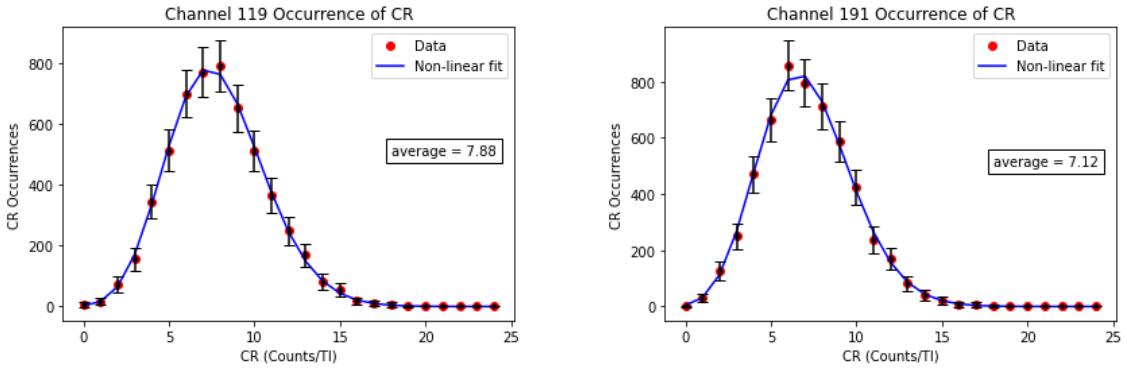

(a) (b)

Figure 2: CR occurrences as a function of CR for the μ=8 counts/TI average experimental run (a) channel 119 with μ=7.88 $\pm$ 0.09 counts/TI (absorption channel) and (b) channel 93 μ=7.12 $\pm$ 0.10 counts/TI (absorption channel). As can be noted again, the average rests around μ=8 counts/TI. These two channels are absorption channels meaning on a Mössbauer spectrum graph, they correspond to dips on the spectra. The blue lines represent the non-linear Poisson fit through the data with black error bars scaled by 3 for visibility.

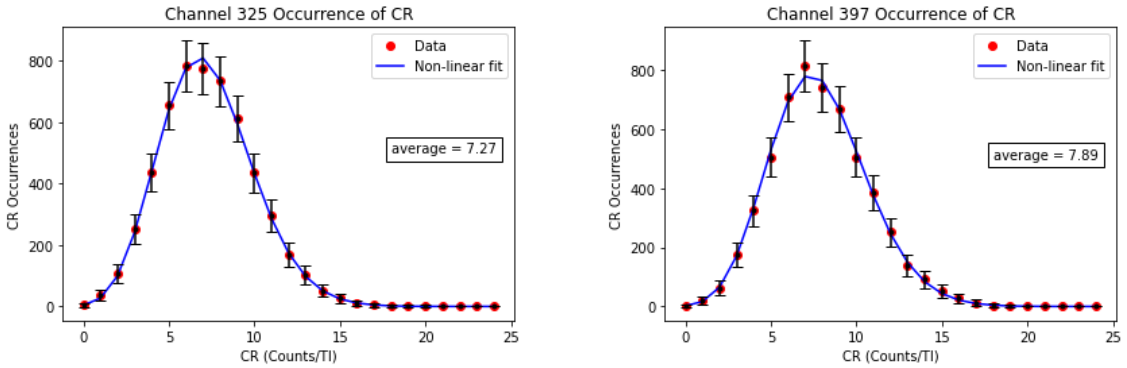

(a) (b)

Figure 3: CR occurrences as a function of CR for the μ=8 counts/TI average experimental run (a) channel 325 with μ=7.27 counts/TI (absorption channel) and (b) channel 397 μ=7.89 counts/TI (absorption channel). These two channels are absorption channels meaning on a Mössbauer spectrum graph, they correspond to dips on the spectra. The blue lines represent the non-linear Poisson fit through the data and the black error bars scaled by 3 for visibility.

the same occurrence of CR graph.

Using this procedure, one can recreate a graph of the average count rates CR as a function of every channel. Whilst the above figure 4 "MFP" graph shows the occurrences of different CRs and the Poisson fits for all 512 channels, figure 5(b) shows the average count rates CR for each channel. An immediate remark is then that figure 5(b) has the same shape as a

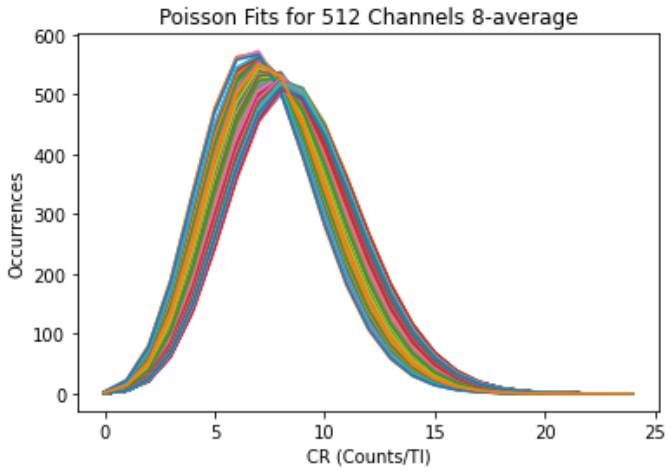

Figure 4: The non-linear Poisson fitting procedure performed on all 512 channels, where each colored line represents the Poisson fit for different channels; from channel 0 all the way to channel 511. We showcased, individually, 6 channels with their corresponding occurrence graphs and Poisson non-linear fits; here in this figure we simply put together all the Poisson fits unique to each channel on the same occurrence of CR graph. As can be noted, the average is yet again around μ=8 $\pm$ 1 counts/TI. This fitting procedure for all channels is called the Mean-fit-Poisson "MFP".

Mössbauer absorption spectrum which can be compared to figure 5(a). This makes sense since for the absorption channel dips, there is generally less occurrences happening than for the background channels. The result obtained here can be compared to figure 9, which shows the result found in the Greek paper.

Besides being the first stepping stone of this project, it can be noted that the new way in which the data was collected allowed us to recreate such graphs, in a way where each channel can be observed and spliced out. Since each data was collected in discrete time steps resulting in thousands of files, one can create programs and codes that can run through these bulk data sets in a way which makes it possible to scrutinize each channel separately. This can't be done nearly as easily for the conventional data collection of Mössbauer spectra since the resulting data set is usually one file at best, which makes going through the whole history of the spectrum much harder. An importance of this technique is therefore that

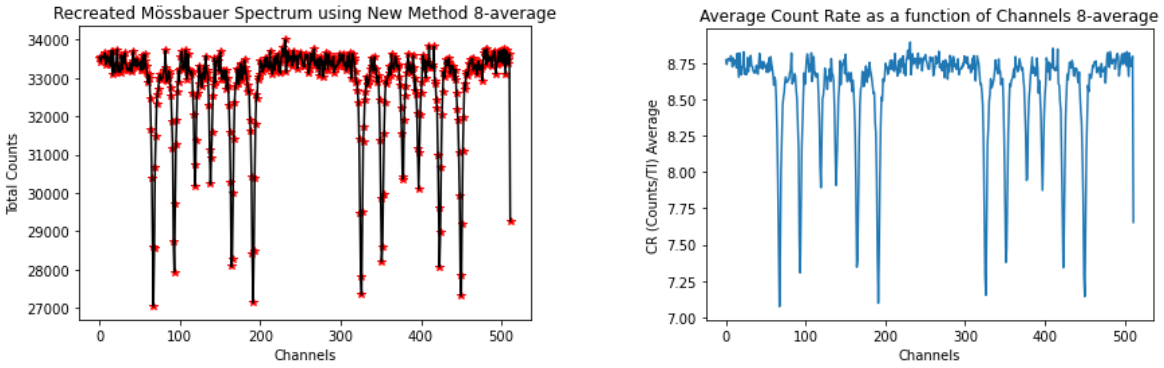

(a) (b)

Figure 5: (a) Recreated Mössbauer absorption spectrum using the MFP method. This recreated spectrum was achieved by simply summing up all the occurrences of each individual channel and turning them into total counts. As can be observed, the spectrum is perfectly in shape with a regular Mössbauer spectrum, and (b) the graph of average CRs as a function of channels.

3.2 The Probability Mass Function and Cumulative Distribution Function spectra estimations "PMF" and "CDF"

Having the capacity to run through thousands of files and to manipulate and separate different data sets in whatever desired way opens up another tool of statistical estimation and analysis. Whilst the mean value of count rates per channel is a generally pertinent information, another good way of looking at the data is to splice between different ranges of count rate CRs for each channel. To make this concept more clear, we shall look at an example. As an illustration, let us look at figure 1(a) for the occurrence graph of channel 50. The mean value of this channel is, as expected, around μ=8 counts/TI. However, we can inquire what the occurrences for a certain discrete range of CR values could be. This is essentially done by picking a starting CR value, called CR1 and an ending CR value, called CR2; then totalling all the occurrences that fall within this range of CR, where the range of CR is the interval between CR1 and CR2.

This is done for all channels, and to illustrate this concept and make it more concrete, an example is given using the channel 50 occurrence graph. For figure 6(a), the action taken is to collect all the occurrences and sum them from CR=0 counts/TI to CR=4 counts/TI; we call this range the 0-4 range. This is also done for figures 6(b) and (c); ranges 7-9 and

8-21 respectively. This specific example is done only for one channel, however we wish to replicate this procedure for all 512 channels. This way, we can recreate an occurrence vs channel spectrum for the different ranges. An example for a various amounts of ranges is provided in figure 12.

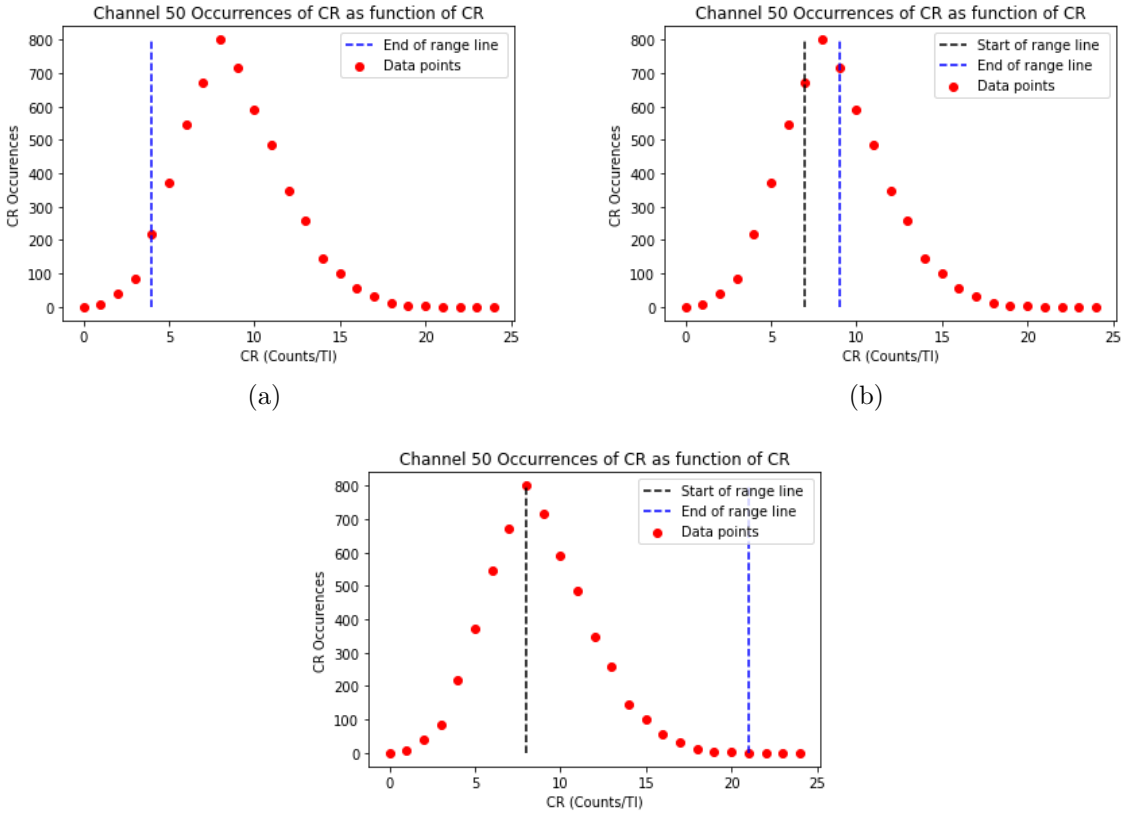

Figure 6: Example of the mechanics going behind the meaning of CR ranges; (a) all occurrences before CR=4 counts/TI and after CR=0 counts/TI are summed, (b) all occurrences before CR=9 counts/TI and after CR=7 counts/TI are summed and (c) all occurrences before CR=21 counts/TI and after CR=8 counts/TI are summed.

It can be now demonstrated that the Mössbauer absorption spectrum can be spliced into multiple different pieces as shown in figure 7. This opens up an elegant way of digging into the data that hides behind the Mössbauer spectra. Such an action would not be quite possible with the conventional collection of data for the absorption spectrum, whereas since the new method collected data in discrete steps, it allows for the reconstruction of the different pieces that ultimately make up a Mössbauer spectrum. A takeaway from this could be that performing such an action where a data set is split into different building blocs might allow

for the possibility to filter noise or background contribution. This protocol of splicing spectra data into different ranges in figure 12 can be compared to that done in the Greek paper in figure 11. Of noted interest for the case where we are dealing with the average count rate μ=8 counts/TI is 12(d), which is the spectrum estimation in around the mean.

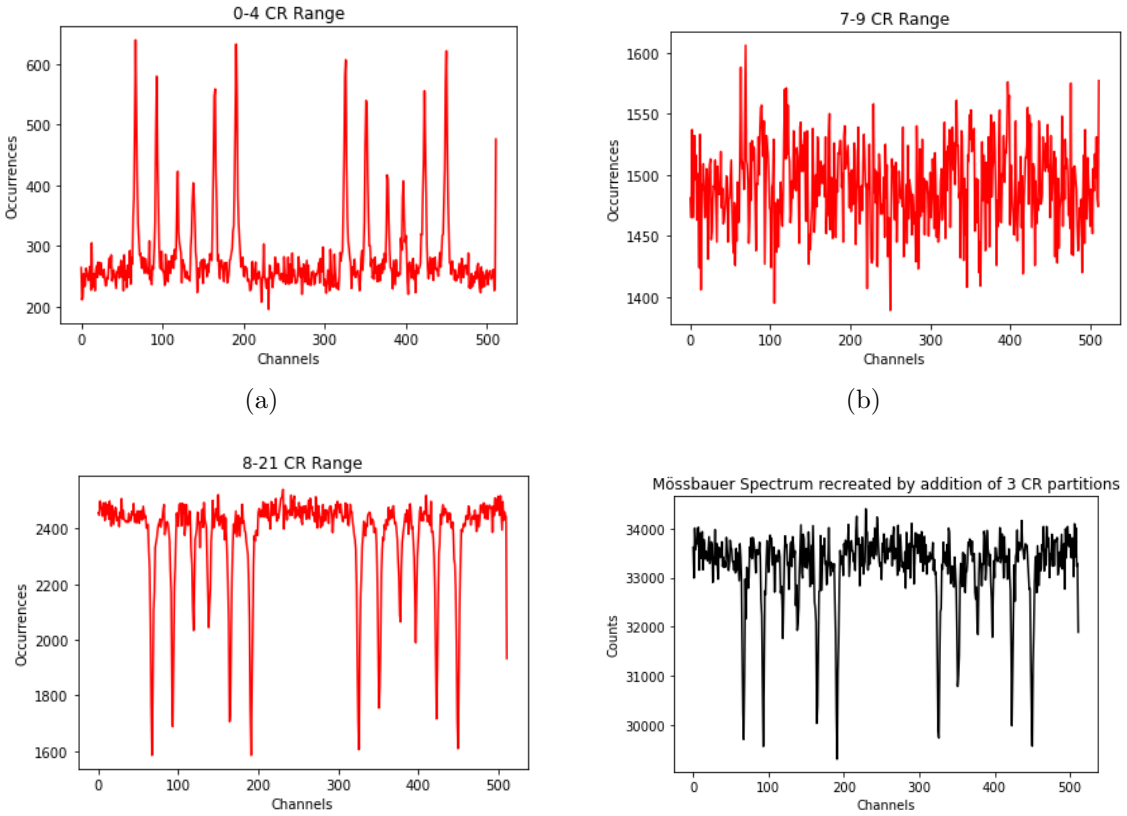

Figure 7: Occurrence vs channels graphs for (a) low CR range 0-4, (b) central CR range 7-9, and (c) high CR range 8-21 counts/TI CR for all 512 channels of the 8 counts/TI experimental run. The final result in (c) is obtained by multiplying the occurrence values of every channel for all three graphs to get the count values in order normalize the y-axis from occurrence values to total counts and then performing a summation of the 3 partition CR ranges; effectively recreating the Mössbauer absorption spectrum we have come to be familiar with. This in effect shows how the Mössbauer spectrum can be split into partitions, or in other words the whole history of the Mösbauer spectrum can be dissected into three distinct pieces.

4 Conclusion

To conclude this paper, the main objective of reconstructing the ALGO algorithm software was not achieved successfully. Despite this fact however, this paper attempted to offer a new way of analyzing and collecting Mössbauer spectra data. The new method of collecting data in discrete steps to obtain a bulk of data sets as opposed to just one data set in the conventional method was shown to have more promising results; by the mere fact that it allowed us to perform more statistical analysis. Indeed the new way in which the data was collected gives more freedom to manipulate and go through data, giving way to analyzing data for each channel for the whole history of the Mössbauer absorption spectrum. Therefore, as the intended goal was not achieved, it is hoped that the paper would help clear the path in some ways through the explanation of each of the steps to allow for a better more focused investigation of this algorithm for future research efforts on the matter. However, one can still conclude that despite this paper's inability to reach the final outcome, the way in which the data was analyzed throughout this project had a better advantage over the conventional method since the data came in a bulk set of information and as such it allowed more freedom in performing statistical analysis.

References

[1] A. Polymeros and A. P. Douvalis, "An alternative statistical approach to the collection and processing of mössbauer spectroscopy data," *The European Physical Journal Plus*, September 2020. [Online]. Available: https://link.springer.com/article/10.1140/epjp/s13360-020-00778-x#Abs1 1, 3, 4

A Appendix 1

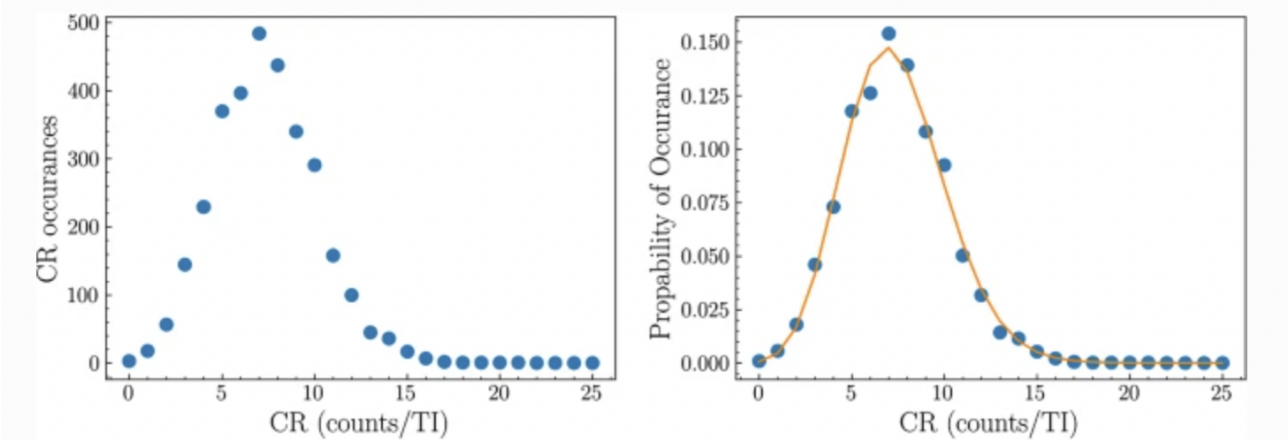

Figure 8: Results of the Greek paper occurrence graph for reference.

B Appendix 2

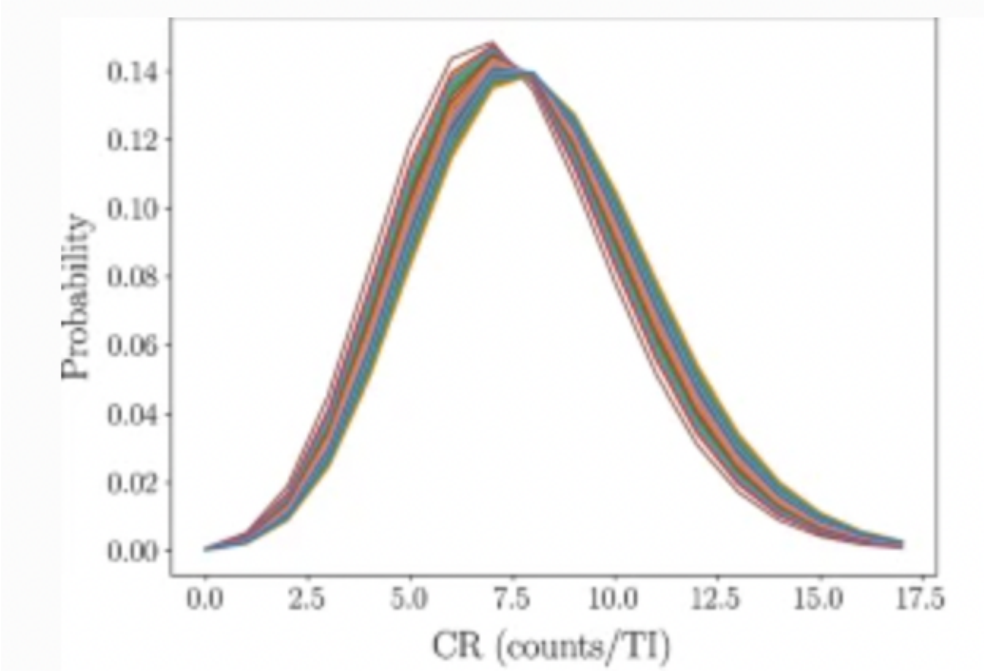

Figure 9: Results of the Greek paper MFP graph for reference.

C Appendix 3

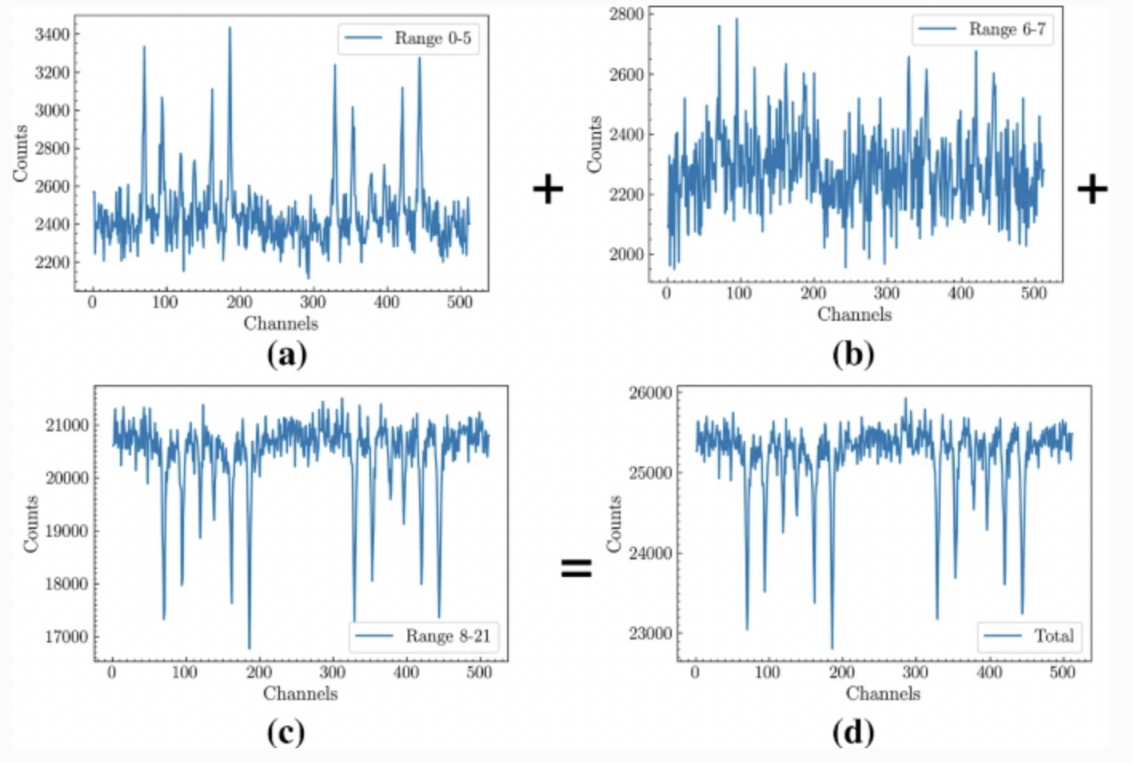

Figure 10: Results of the 3 partial summations of the Greek paper for reference.

D Appendix 4

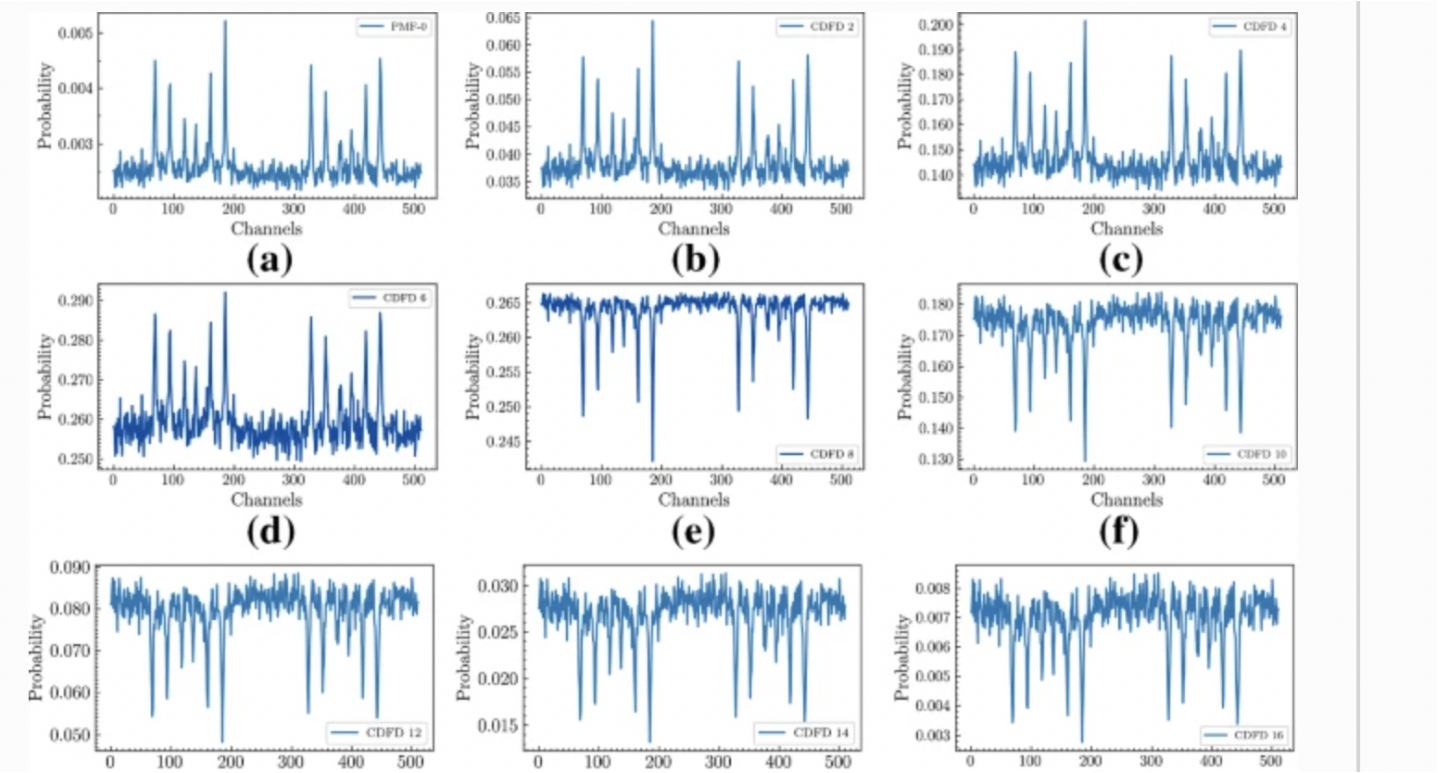

Figure 11: Results of the different ranges of the Greek paper for reference.

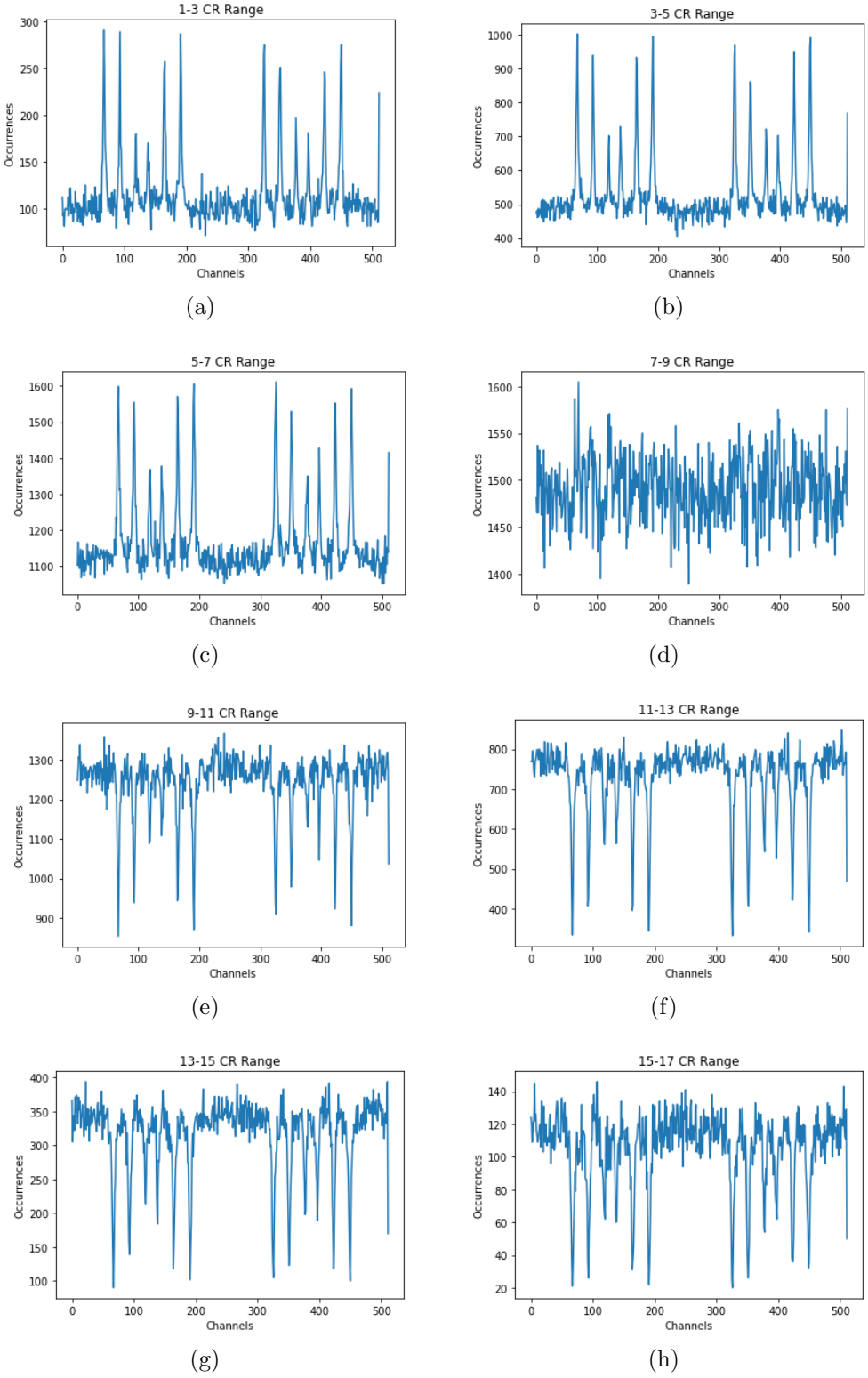

Figure 12: A gallery of different ranges of CR from very low, to central to high CR ranges showcasing the use of the Cumulative Distribution Function method (CDF). The ranges are the partial summed occurrences for a given interval of CRs for all 512 channels for the 8 counts/TI average experimental run.

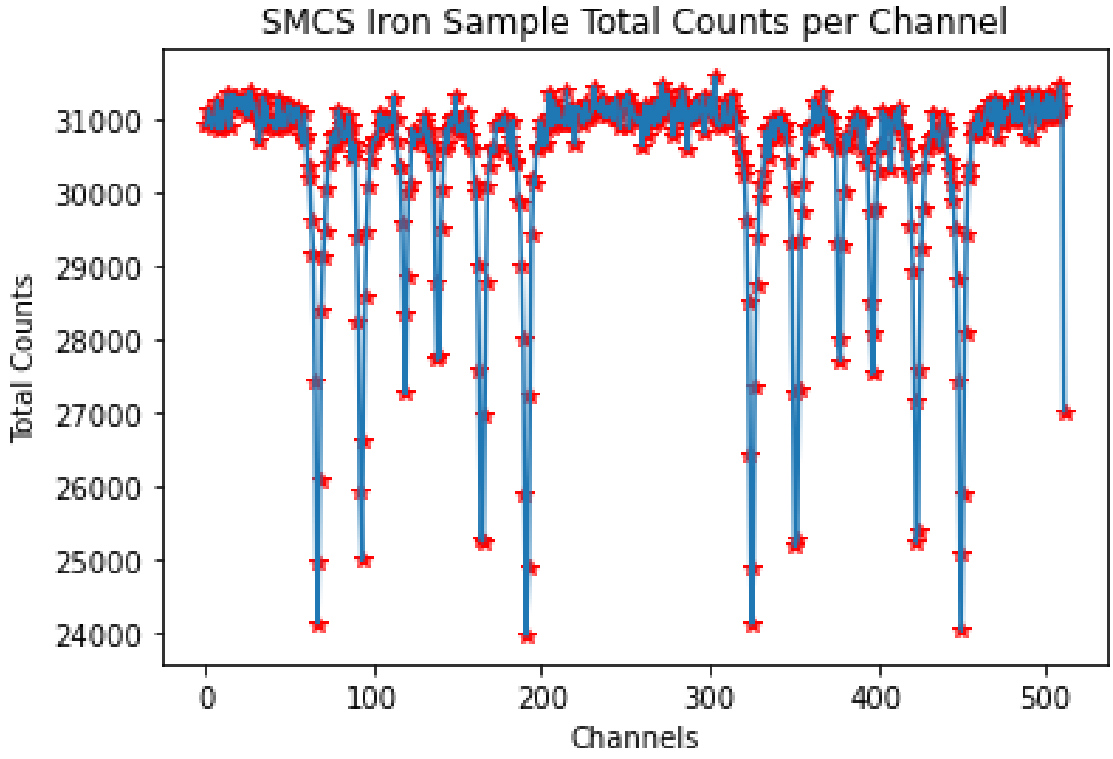

Figure 13: A typical Mössbauer spectrum graph obtained using conventional data collection.